

## KRZYSZTOF DUDA, ANDRZEJ BIENÍ

AGH University of Science and Technology  
Measurement & Instrumentation Department  
Krakow, Poland  
e-mail: kduda@agh.edu.pl, abien@agh.edu.pl

### DIGITAL MEASUREMENT OF TRANSIENT DISTURBANCES IN ELECTRIC POWER NETWORK WITH ADDITIONAL LOWPASS ANALOG CIRCUIT

The paper presents a DSP-based system for measurement of the short-term transient distortions in electric power networks. These distortions typically possess short duration times and high amplitude values and thus they are very difficult to acquire by standard digital data acquisition systems. We propose to apply an additional analog lowpass  $RC$  circuit before digital data acquisition. A properly chosen analog  $RC$  filter extends the duration time of transient distortion and simultaneously reduces its amplitude making it significantly simpler to acquire digitally. Next, digital signal processing is used for cancelling the analog convolution of the acquired signal with a  $RC$  filter. The paper discusses results obtained for different configurations of the proposed measurement system including  $RC$  filter selection and digital deconvolution filter design. The algorithm was implemented in a Texas Instruments C617 DSK toolkit. Laboratory experiments with voltage signals are presented in the paper.

Keywords: transient distortion measurement, DSP system, Power Quality monitoring

#### 1. INTRODUCTION

Transient disturbances are an important Power Quality factor of the electric power network. They are characterized by short duration times (compare to the 20 ms period of a 50 Hz component), typically less than 1 ms and high values of amplitudes, over 10% of mains voltage. The main source of transient disturbances is the load switching effect in an inductive electricity grid. In spite of containing small energy, transient disturbances cause significant malfunctioning especially in electronic, but also electric equipment.

Power Quality estimation requires detection and measurement of transients. Typically it is provided by counting the number of transients exceeding a predefined threshold. We propose both transient detection and measurement of its parameters (maximum value, duration time and energy). We use analog preprocessing of the signal with lowpass  $RC$  filter, what let us to better use the dynamic range of the AD converter.

Simultaneously a lowpass  $RC$  filter provides additional over-voltage protection of the AD converter and the possibility of sampling frequency rate reduction.

## 2. MEASUREMENT SYSTEM AND PROPOSED INSTRUMENT

The instrument is ready to use in a low voltage (230V) measurement system. The structure of the instrument is presented in Fig.1. The separating voltage transformer is the input of the instrument. Two main functions of this transformer are: 1) reducing the input voltage and 2) over-voltage protection of the user, it also eliminates DC component. The next stage is a lowpass  $RC$  passive filter followed by the A/D converter. The acquired digital voltage signal is processed by a microcontroller or DSP system. The overall output is available as graphic human interface (the results are presented on computer screen as time plots) and serial computer interface (for storage and communication or/and further analysis by another computer system).

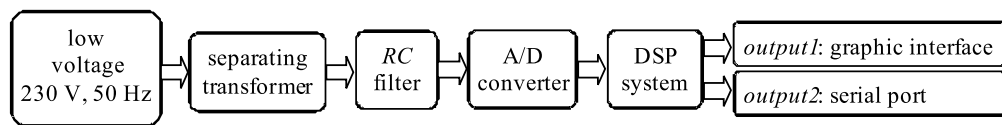


Fig. 1. Block diagram of the instrument in a measurement system.

### 2.1. Analog lowpass filter

A block diagram of the measurement system tested in the laboratory is depicted in Fig. 2. The main idea is to use an analog lowpass filter  $H_a(s)$  before digital signal processing. The Laplace transform of analog filter is given by:

$$U_c(s) = U(s) \frac{1}{sRC + 1} = U(s)H_a(s). \quad (1)$$

For the analog  $RC$  circuit  $R = 2 \text{ k}\Omega$  and  $C = 470 \text{ nF}$  were chosen. After calibration of the system the correction was computed and the value of  $RC = 952 \cdot 10^{-6} \text{ s}$  was estimated, the amplitude of the 50 Hz component for that  $RC$  value is practically not affected (50 Hz attenuation is 0.96) and the integration of the input voltage  $U_{in}$  is sufficient. The amplitude characteristic of this filter is depicted in Fig. 3a. After acquiring voltage  $U_c$ , the objective of the digital part of the system is to compute the output voltage  $U_{out}$  such that ideally for time signals the condition:

$$U_{out} = U_{in}, \quad (2)$$

is fulfilled or such that Eq. (2) should be satisfied as well as possible (in least squares error sense) with neglecting time delay caused by digital signal processing. To complete this task, by means of digital convolution, the digital filter  $H(z)$  should be designed with an amplitude characteristic inverse to the analog filter  $H_a(s)$  which means:

$$abs(H_a(j\Omega))abs(H(e^{j\omega})) = 1, 0 < \{\Omega = \omega\} < \Omega_s/2, \tag{3}$$

where:  $\Omega$  – analog frequency [rad/s],  $\omega$  – digital frequency [rad/s],  $\Omega_s$  – sampling frequency [rad/s]. The phase characteristics of both filters were not considered. We designed a number of digital filters according to condition (3), but as they performed with similar results, the next section describes only two design cases: bilinear transform and yulewalk method.

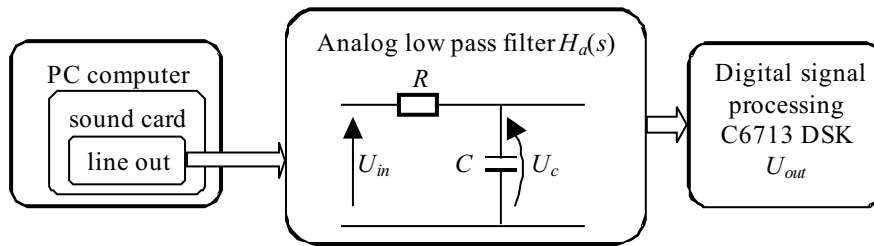


Fig. 2. Block diagram of measurement system as configured for laboratory experiments. PC computer with sound card was used as a signal source.

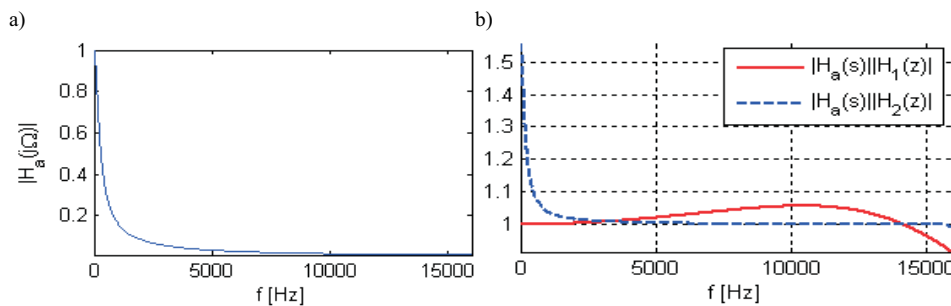


Fig. 3. a) Amplitude characteristic of analog filter  $H_a(s)$  (for 50 Hz, attenuation is 0.96), b) Quality of inverse digital filters  $H_1(z)$  and  $H_2(z)$  in sense of condition (3).

### 2.2. Digital inverse filter

The first approach to inverse digital filter design was to apply bilinear transform to  $H_a(s)$  and to take the inverse transmittance of the resulting discrete filter. Unfortunately

as  $H_a(s)$  has a zero in infinity the resulting discrete filter has a zero in  $-1$  and is not minimum phase, thus it cannot be inverted. We checked the properties of the inverse filter with zero of transmittance moved from  $-1$  toward zero on the  $Z$  – plane and find surprisingly good results in sense of condition (3). The final location of zero for this inverse discrete filter denoted as  $H_1(z)$  is depicted in Fig. 4 and the condition (3) for this case is presented in Fig. 3b (continuous line).

The second digital inverse filter denoted as  $H_2(z)$  was designed with a least squares fit to a specified frequency response (function *yulewalk* from Matlab Signal Processing Toolbox). Desired frequency response was evaluated upon the characteristic of analog filter  $H_a(s)$ . The zero-pole plot of this filter is depicted in Fig. 4c and condition (3) is shown in Fig. 3b (dotted line).

Both filters are IIR with orders 1 and 16 respectively. The condition (3) can be also fulfilled with a FIR filter of 16-th order but the impulse response of such a FIR filter is too long and during experiments it was the cause of oscillations that could not be accepted. In contrast, IIR filters possess infinite impulse response, but with fast decay. As seen from Fig. 4b,d the samples of impulse response above 5-th are negligible.

The zeros poles values and gains values for both filters are given in Table 1.

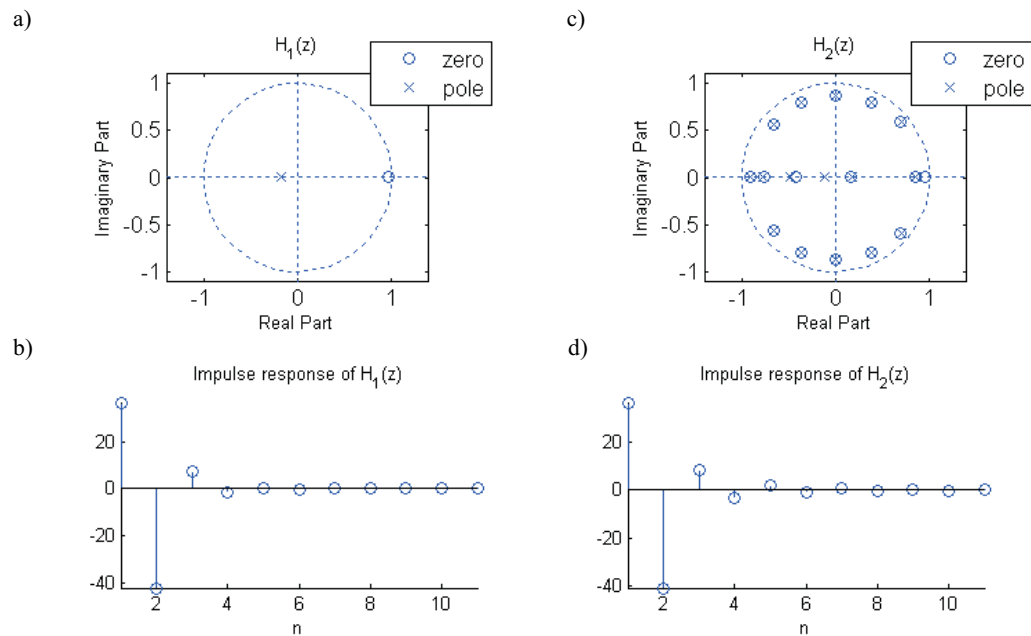


Fig. 4. Inverse digital filters  $H_1(z)$  and  $H_2(z)$ . Zero – pole plots of transmittances and impulse responses.

Table 1. The zeros poles values and gains values for filters  $H_1(z)$  and  $H_2(z)$  (compare Fig. 4 a,c).

	zeros	poles	gain
$H_1$	0.96772311	-0.18000000	36.55866560
$H_2$	0.95246430	0.85188120	36.29623499
	0.84624918	0.69703036 + 0.59273063i	
	0.69692678 + 0.59274706i	0.69703036 - 0.59373063i	
	0.69692678 - 0.59274706i	0.38391879 + 0.80350240i	
	0.38380955 + 0.80347463i	0.38391879 - 0.80350240i	
	0.38380955 - 0.80347463i	0.00516384 + 0.87505744i	
	0.00505074 + 0.87504904i	0.00516384 - 0.87505744i	
	0.00505074 - 0.87504904i	-0.37001863 + 0.79882362i	
	-0.37008596 + 0.79882658i	-0.37001863 - 0.79882362i	
	-0.37008596 - 0.79882658i	-0.66259142 + 0.56491714i	
	-0.66265942 + 0.56488363i	-0.66259142 - 0.56491714i	
	-0.66265942 - 0.56488363i	-0.90750163	
	-0.90552927	-0.77645553	
	-0.76561734	-0.48415048	
-0.41986175	0.18230039		
0.16352098	-0.11828020		

### 2.3. DSP implementation

Both inverse digital filters described in section 2.2 were implemented in the Texas Instruments C6713 DSK toolkit with floating point precision (32 bit accumulation and 40 bit multiplication). This platform has support from the Matlab Simulink environment. The block diagram of signal flow in algorithm is depicted in Fig. 5. The chosen sampling frequency value was  $F_s = 32$  kHz. *Channel1* was used for processing voltage  $U_c$  and *Channel2* for monitoring voltage  $U_{in}$  (denotations from Fig. 2). The analog output of the system was used for connecting an oscilloscope during test time.

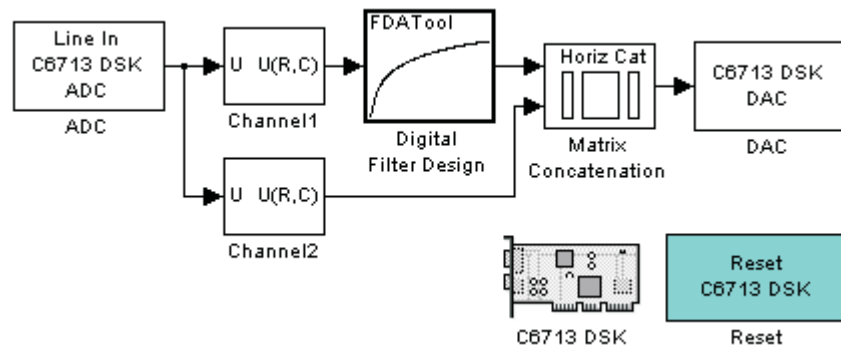


Fig. 5. Simulink block diagram of the digital signal processing part of the measurement system implemented in C6713 DSK. Sampling frequency  $F_s = 32$  kHz, *Channel1* is used for acquisition of  $U_c$  and *Channel2* is used for acquisition of reference signal  $U_{in}$ .

## 3. EXPERIMENTAL RESULTS

Experiments took place in a laboratory with voltage signals. As depicted in Fig. 2, the sound card of a PC was used as the signal source which gave the possibility of generating practically arbitrary signal shapes (arbitrary distortion). The signal was next played as a wave file. Examples of measurement system performance are depicted in Fig. 6. The presented data were taken from C6713 DSK memory via Code Composer Studio. The left column in Fig. 6 shows one period of 50 Hz sinusoid whereas the right column is zoomed in on transient distortion. Rows in Fig. 6 present results for filters  $H_1(z)$  and  $H_2(z)$  described in section 2.2. As seen from Fig. 6b, d, voltage  $U_{out}$  computed from  $U_c$  shows good similarity with  $U_{in}$  and  $U_c$  practically does not exceed the amplitude range of 50 Hz, although  $U_{in}$  significantly does. The errors computed for signals from Fig. 6b, d, defined as  $\varepsilon_1 = 100 \cdot \text{mean}\{|U_{in} - U_{out}|/\max(U_{in})\}$  and  $\varepsilon_2 = 100 \cdot (\max(U_{in}) - \max(U_{out}))/\max(U_{in})$  took values  $\varepsilon_1 = 4.6\%$  and  $\varepsilon_2 = 8.1\%$  for Fig. 6b, and  $\varepsilon_1 = 5.4\%$ ,  $\varepsilon_2 = 0.7\%$  for Fig. 6d.

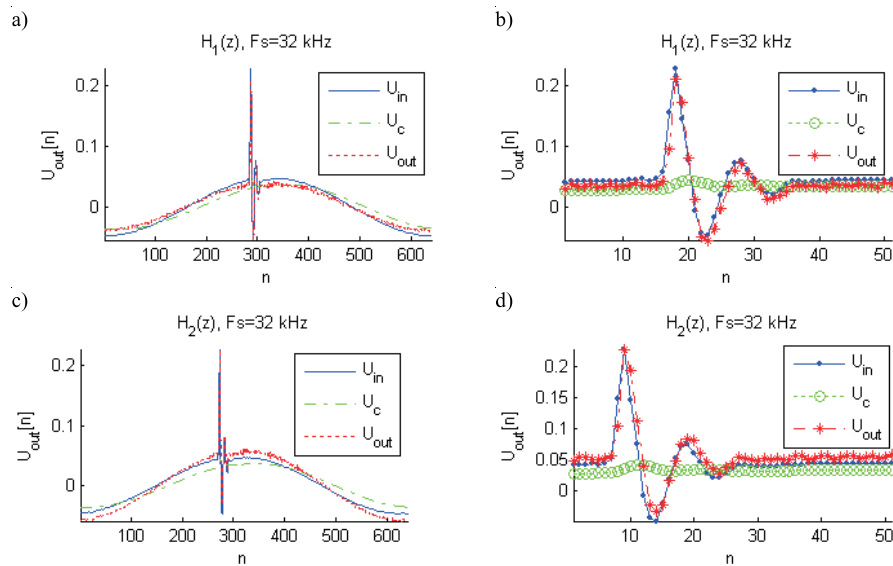


Fig. 6. Results of experiments conducted in a laboratory (data from DSP memory). Left column shows a 20 ms observation (one period of 50 Hz). The right column shows the same signals zoomed in to 1.6 ms observation. Duration time of the distortion is about 25 samples (0.8 ms). Rows show results obtained with different digital filters  $H_1(z)$  and  $H_2(z)$  (see section 2.2 for details).

#### 4. CONCLUSIONS

The input analog circuit introduced in a digital measurement system as depicted in Figs. 1, 2 has the following advantages:

- 1) It enables acquiring transient disturbances with peak magnitude significantly exceeding the range of the A/D converter,
  - 2) Duration time of transient disturbances after lowpass filtering significantly increases what allows to use a lower sampling frequency,
  - 3) The input analog lowpass circuit reduces noise disturbances during data acquisition.
- All these advantages were verified in a set of experiments conducted in the laboratory with implementation in the Texas Instruments C617 DSK toolkit.

As the digital part of the proposed measurement system consists only of a digital IIR filter (with possible order 1) the algorithm is computationally cheap and can be part of a bigger Power Quality monitoring system, or can exist independently in a low cost DSP system.

Presented results obtained for floating point precision are comparable for both IIR filters, thus the first order filter seems to be reasonable choice, whereas for fixed point precision quantization errors should be additionally considered in both cases.

#### REFERENCES

1. Signal Processing Toolbox For Use with MATLAB. User's Guide Version 6, [www.mathworks.com](http://www.mathworks.com)
2. Duda K., Bień A.: *Real-time detection of transient disturbances in electric power network*, 14<sup>th</sup> IMEKO TC4 Symposium on New Technologies in Measurement and Instrumentation and 10<sup>th</sup> Workshop on ADC Modelling and Testing, Jurata – Gdynia, Poland.
3. Duda K., Bień A.: *Design of a recorder of quick-changing disturbances in a power network*. XV<sup>th</sup> Symposium of Measurement Systems Modeling and Simulation, September 18-22<sup>nd</sup>, Krynica (in Polish).
4. Duda K., Bień A.: *Digital measurement of pulse disturbances in a power network using analog integration – experimental investigation*. XVI<sup>th</sup> MiSSP Symposium 2006 (in Polish).
5. Ptasieński L. Żegleń T.: *Ignition investigation of methane-air mixtures by multiple capacitor discharges*, 9<sup>th</sup> international conference on Electrostatics, Electrostatics 2001, Zakopane, 29.V.2001.
6. Zieliński T.: *From theory to digital signal processing*. WKŁ, Warsaw 2005 (in Polish).
7. Leonardo Power Quality Initiative, [www.lpqi.org](http://www.lpqi.org)